Monthly Notices
of the
ROYAL ASTRONOMICAL SOCIETY
MNRAS **480,** 2137–2143 (2018) doi:10.1093/mnras/sty1942

Stellar activity of evolved, cool giants – old questions revisited

K.-P. Schröder,[1★] J.H.M.M. Schmitt,[2★] M. Mittag,[2] V. Gómez Trejo[1] and D. Jack[1]

[1] *Depto. Astronomía, Universidad de Guanajuato, A.P. 144, Guanajuato, GTO, C.P. 36000, Mexico*
[2] *Hamburger Sternwarte, Universität Hamburg, Gojenbergsweg 112, D-21029 Hamburg, Germany*

Accepted 2018 July 15. Received 2018 July 13; in original form 2017 October 24

ABSTRACT

We present an empirical study of the strength of magnetic stellar activity among cool giant stars on the red and asymptotic giant branches using the Ca II H&K chromospheric emission strength measured in the context of the Mount Wilson project. Because we consider only stars with a parallax error smaller than 10 per cent, the stars can be accurately placed into an empirical Hertzsprung–Russell diagram and their evolutionary status can be reliably assessed from a comparison with calibrated evolutionary tracks. We find that *S*-index values among evolved giants redder than 1.5 in $B - V$ and with luminosity classes I and II are larger than those found among the progenitor K giants with luminosity class III and $B - V < 1.3$. Converting the measured *S*-indices into physical chromospheric surface fluxes, we find that chromospheric heating undergoes a remarkable reversal and revival as giant luminosity increases. We also discuss possible explanations for this new finding.

Key words: stars: activity – stars: chromospheres – supergiants.

1 INTRODUCTION

One of the early discoveries in activity studies of late-type stars was that of a dividing line in the Hertzsprung–Russell (HR) diagram, which separates solar-like stars with chromospheres and transition regions from non-solar-like stars without any indications of transition regions but substantial mass loss (Linsky & Haisch 1979). A little later, the concept of a dividing line was extended into the X-ray range, when Ayres et al. (1981) showed that indeed – as expected by Linsky & Haisch (1979) – the presence of transition region material detected, for example, in C IV λλ 1548 formed at temperatures of $\approx 10^5$ K, goes along with X-ray emission formed at temperatures $> 10^6$ K. The X-ray dividing line derived by Ayres et al. (1981) rises diagonally from about spectral type K2 III to warmer effective temperatures at higher luminosities.

This dividing line is usually interpreted as the disappearance of stellar activity, when mass loss sets in, in the form of a cool wind (see Hünsch & Schröder 1996, and references therein). Evolutionary arguments, such as more efficient magnetic breaking in cool giants, made this explanation appear plausible (see Schröder, Hünsch & Schmitt 1998), especially as the observed dividing line is perpendicular to the evolutionary tracks of cool giants on their red giant branch (RGB) and asymptotic giant branch (AGB), widened only on the temperature scale by a variation in mass and metallicity.

However, this picture has never become fully consistent with all observational findings. Reimers (1982) has already pointed out the existence of giants, which feature ultraviolet (UV) spectroscopic evidence for both a cool wind seen in the Mg II h&k lines, and a hot transition region type plasma emitting in the C IV and Si V lines, thus suggesting the existence of embedded coronal plasma. These stars were then consequently called hybrid stars, clearly presenting an uncomfortable contradiction to the general picture of declining activity on the cool side of the HR diagram. In deeper X-ray observations with *ROSAT*, coronal X-ray emission was found from most of the hybrid stars studied by Reimers & Schmitt (1992), Kashyap et al. (1994) and Hünsch et al. (1996), yet these giants were seen as atypically active exceptions to the general picture of declining activity on the cool side of the HR diagram.

Ayres et al. (1997) – and precursors to that publication – then developed the view that the disappearance of coronal emission among cool giants beyond the dividing line does not imply the absence of any stellar activity but, rather, the activity is simply not observed in the same way as we know it from the normal, solar-type stars. This scenario was given the names ‘coronal graveyard’ and ‘buried alive’ magnetic fields (Ayres, Brown & Harper 2003), where the much larger pressure scaleheights lead to magnetic loops being covered under chromospheric gas. Therefore, X-ray non-detections do not necessarily give the correct picture of stellar activity among very cool giants.

There are a number of reasons to support this point of view, beyond those given at the time by Ayres et al. (1997). A key finding from a purely empirical point of view is the direct detection of magnetic fields in the photospheres of cool, evolved giants presented by Konstantinova-Antova et al. (2013) and Aurière et al. (2015), inspired by the pioneering work of Hubrig et al. (1994). Using spectropolarimetry over the entire visible spectrum, magnetic fields

★ E-mail: kps@astro.ugto.mx (K-PS); st8h101@hs.uni-hamburg.de (JHMMS)

can be measured with a sensitivity in the range of a few gauss, and observations of a larger sample of evolved cool giants advancing on the RGB and AGB demonstrate that magnetic fields in the photospheres of cool giants are, indeed, not the exceptional case, but rather an entirely common and normal phenomenon. Specifically, Aurière et al. (2015) report the detection of magnetic fields in 29 out 48 giants that were observed in their Zeeman survey; in the subsample of 24 giants with previously known signatures of activity, 23 stars were also detected to have magnetic fields. Clearly, this evidence points to a close connection between activity and magnetic fields and it avoids the above-mentioned bias of coronal detections among cool giants.

The only other useful activity indicator in this respect is chromospheric emission. While a large amount of knowledge on chromospheres has been gained by studies based on *IUE* and *Hubble Space Telescope* (*HST*) UV spectra, utilizing the rich UV emission-line spectrum of the chromospheres of cool stars, the widest coverage in terms of stars has actually been achieved by ground-based observations of the Ca II H&K line emission. Such observations can be carried out by spectroscopy (with a resolution of 20 000 or better) on even modest-sized telescopes. Its direct relation to solar and stellar magnetic activity had already been discovered very early on by Eberhard & Schwarzschild (1913) and was extensively studied by O. C. Wilson for decades. In the 1960s, Wilson finally developed a quantitative measure of the Ca II H&K emission strength, the so-called *S*-index, and began a systematic chromospheric activity monitoring programme, using the 2.5-m and, later, 1.5-m telescopes at the Mount Wilson Observatories; we refer to Vaughan, Preston & Wilson (1978), Wilson (1978), Duncan et al. (1991) and Baliunas et al. (1995) for more details on the hardware used, a presentation of key observational results and for further references.

However, at the time of the presentation of those results in the 1990s, the scientific impact of the Mount Wilson programme was limited, considering the huge effort that had gone into it. With hindsight, we can identify three reasons for this. First, the *S*-index is an ingenious activity measure in the sense of its independence from observational or stellar conditions and in its timeless way of calibration, but it was difficult to compare in absolute terms with the flux measurements obtained by satellites such as the *IUE*, despite efforts by Rutten (1984) and Rutten et al. (1991). This problem was solved only recently by calibrating against model atmospheres; see Mittag, Schmitt & Schröder (2013) and Pérez Martínez, Schröder & Hauschildt (2014) for more details. Secondly, exact parallaxes were not available at the time and, consequently, the Mount Wilson project *S*-data were published without any quantitative astrophysical perspective. Thirdly, the untimely loss of the project leader in 1994, limited funding and insecure science careers of the remaining team members had the consequence that these shortcomings were never addressed, once *Hipparcos* parallaxes became available (see Perryman 2002).

The new findings of Konstantinova-Antova et al. (2013) and Aurière et al. (2015), as well as the exploration of our own new chromospheric activity data obtained with our TIGRE telescope (Schmitt et al. 2014), have inspired the work presented here. Aurière et al. (2015) give convincing evidence for an increase of magnetic field strength detected in the photospheres of a selected sample of evolved giants with the ascent on the AGB and RGB. In addition, with *S*-indices derived from their own data, these authors demonstrate a good, albeit scattered, correlation between chromospheric emission and magnetic field strength (see fig. 10 of Aurière et al. 2015). Still, the sample used by Aurière et al. (2015) is limited in size. Here we present empirical evidence for the evolution of stellar activity, in particular in the later giant stages, using only *S*-indices rather than detailed spectra as chromospheric activity indicator, but measured for a large number of stars with well-determined positions on the HR diagram, which can be compared to a well-calibrated grid of evolutionary tracks.

2 WHY DO MOST EVOLVED, COOL GIANTS LACK CORONAE?

To better understand the above-mentioned bias of coronal X-ray detections and their failure as a probe into the distribution of stellar activity for evolved cool giants, we point out two important findings.

First, chromospheric eclipse observations of ζ Aur-type binaries across the Linsky–Haisch coronal-wind dividing line in the HR diagram show a dramatic growth of their chromospheric extents (see Schröder 1990, and figs 3 and 4 in that paper). ζ Aur systems are eclipsing binaries consisting of a late-type giant and a hotter companion. Because of their specific geometry, they directly provide an observable height resolution of their chromospheres, when during an eclipse the hot binary companion is shining through the giant's chromosphere from behind and is scanning the giant's chromosphere moving along its orbit. For this sample of giant stars, this demonstrates a substantial physical change in their outer atmospheres.

Secondly, inactive stars on the coronal side of the Linsky–Haisch division (Linsky & Haisch 1979) – that is, those stars not showing any magnetic heating related chromospheric emission beyond the basal flux – nevertheless show a kind of basal coronal X-ray luminosity, comparable to the X-ray surface flux of the inactive solar corona (Schmitt 1997). In their survey of nearby giants, Hünsch et al. (1996) find a plateau of X-ray emission near an X-ray luminosity L_X of 10^{27} erg s^{-1} or $L_X/L_{bol} \approx 10^{-8}$ for giants with a $B - V$ colour below 1.2. In contrast, the redder giants typically remain undetected in the *ROSAT* data.

Consequently, taking into account only the large majority of inactive, or less active stars (and so for the moment excluding the more exceptional and active hybrid stars), the division between coronae and cool winds in the HR diagram found by Linsky & Haisch (1979) is actually well defined and reflects, based purely on observational evidence, a large change in the physical properties of the outer giant atmospheres in this part of the HR diagram. Only very active giants appear as X-ray sources (and hybrid stars) on the more evolved side of the Linsky–Haisch division.

Given this complexity, is it possible to understand this change with simple arguments based on chromospheric physics? From the Sun, we are familiar with the so-called Athay description of the transition from the chromosphere to the corona (e.g. Athay & Thomas 1956; Athay 1981). In the very simplest terms, energy is continuously deposited in the chromosphere, but this heating is balanced by radiative cooling from recombination processes. In this way, the large reservoir of neutral hydrogen keeps the chromospheric temperatures stable under about 10 000 K. As plasma densities decrease with height, the hydrogen ionization fraction rises, and so does the reservoir of free electrons to spark collisional excitation, followed by radiative cooling though collisionally excited resonance lines. The larger radiative losses through a larger reservoir of free electrons balance a larger heating rate.

In coronal stars, hydrogen ionization comes ever closer to 100 per cent, so that the free electron reservoir cannot sufficiently grow with a rising heating rate, and radiative cooling becomes unable to balance any stronger heating. In consequence, a runaway process occurs, with the temperature rising very steeply by two orders of magnitude to transition region and coronal values, where finally heat conduction by electrons is able to re-establish a new cooling process and hence thermal equilibrium. Consequently, we can assume that the non-detection of a corona around a cool, inactive star means that its chromosphere does not reach that critical point. At the risk of oversimplification, we would like to highlight two relevant factors to produce this outcome: one works along the luminosity coordinate of the HR diagram, and the other along the $T_{\rm eff}$ coordinate.

For more luminous giants, by applying hydrostatic equilibrium at the temperature minimum (neglecting magnetic terms), Ayres, Shine & Linsky (1975) find that chromospheric column densities $N_{\rm chrom}$ should scale as $N_{\rm chrom} \propto 1/\sqrt{g}$. Because the pressure (and density n_0) at the base of the chromosphere scales with $g\,N_{\rm chrom}$ or, consequently, with $\sqrt{g}$, then scaleheights L in this simple hydrostatic model are increasing up the giant branches with g^{-1}, as roughly $N \propto L\,n_0$. In this way, the well-established Wilson–Bappu effect (Wilson & Bappu 1957; Wilson 1967) is explained mainly by an increasing Ca II K line opacity with decreasing gravity (increasing luminosity).

This simple model is fully consistent with the growing extent of giant chromospheres found empirically by Schröder (1990) and mentioned above. Even though a stellar chromosphere, as we know it from the Sun, is highly magnetically structured, the Wilson–Bappu effect also empirically confirms the simple hydrostatic approach of Ayres et al. (1975). Consequently, any given amount of surface energy flux dissipated into a giant chromosphere has to heat a much larger column density on the evolved side of the Linsky–Haisch division.

In addition, in those giants with a substantial magnetic activity, such larger column densities lead to the tapping of magnetic field loops under dense chromospheric plasma, which is the argument of Ayres et al. (2003). The effect is the same: an absence or a reduction of coronal emission, which is not related to lower activity.

Now, looking at the temperature axis of the HR diagram, the basal chromospheric surface flux $F_{\rm CaII}$, as measured for example in Ca II H&K emission, is observed to decrease steeply (see Pérez Martínez, Schröder & Cuntz 2011; Pérez Martínez et al. 2014). The available data suggest a dependence $F_{\rm Ca\,II} \propto T_{\rm eff}^{7-7.6}$. As most cool giant stars are of moderate activity, their chromospheric Ca II emission flux falls into a relatively narrow (0.5 dex) band between this basal flux and only about three times this flux (see fig. 5 in Pérez Martínez et al. 2014).

In summary, from both observational and theoretical arguments, it appears that coronal emission strongly decreases, or among inactive cool giants even disappears, but this is for reasons unrelated to stellar activity. Consequently, coronal X-ray detection becomes unsuitable as an activity indicator for evolved giant stars. Other, unbiased activity indicators are required. It is for this purpose that we present the following work based on chromospheric Ca II line emission.

3 CHROMOSPHERIC EMISSION: A LESS BIASED INDICATOR OF STELLAR ACTIVITY ACROSS THE HR DIAGRAM

Sensitive measurements of both magnetic fields and chromospheric Ca II H&K emission are good activity indicators in the sense that both avoid the biases of coronal X-ray detections. In addition, chromospheric emission is straightforward to observe and, in fact, because of the Mount Wilson project, such data already exist for over a thousand stars.

3.1 Mount Wilson *S*-index observations

Conventional, ground-based spectroscopy has been performed for many years for many stars. A large body of data on chromospheric Ca II H&K line emission has been observed in the context of the Mount Wilson project, resulting in calibrated *S*-index measurements that are independent of the instrumental details and atmospheric transparency. Unfortunately, using his approach, it is not possible to record surface fluxes in absolute terms.

Without repeating the exact definition of the *S*-index and its calibration (see Vaughn et al. 1978 for an original account), we merely recall that *S*-index values give the chromospheric emission (measured in two narrow windows of about 1-Å width) relative to the strength of the nearby pseudo-continuum (measured in two symmetrically placed 20-Å windows on the blue and red sides of the Ca II doublet, chosen to be less crowded with lines, referred to as *R* and *V* bands).

This idea of the *S*-index was developed by Wilson in the 1960s and used by his research group into the 1990s. Measurements in those days were taken directly on the optical spectrum, using a four-channel photomultiplier, while nowadays the *S*-index is obtained numerically from the digitally recorded and reduced spectrum. What makes these so different approaches fully comparable is the list of *S*-index values for 17 calibration stars used and passed on by Wilson, who selected these stars as a calibration sample in order to provide different, but relatively invariable activity levels. In this way, the *S*-index gives the chromospheric emission in measures of the photospheric flux in the reference windows, which falls towards lower effective temperatures nearly as steeply as the basal and moderately active chromospheric emissions do (as mentioned above; see Pérez Martínez et al. 2014).

Viewed from the observational side, this definition of the *S*-index is of great practical advantage, as the resulting values of, for example, weakly active stars, depend only little on the stellar parameters, such as the effective temperature in particular. In absolute terms, however, this definition requires a careful discussion (see Section 3.3).

3.2 Impact of Wilson–Bappu effect

Another issue with *S*-index measurements of giants is the impact of the Wilson–Bappu effect (Wilson & Bappu 1957), which smears out the Ca II line emission of the more luminous cool giants beyond the nominal 1-Å window, in which the *S*-index is measured and calibrated. In addition, line scattering of the chromospheric emission, produced at the bottom of the chromosphere, into the extended outer chromosphere and wind region of supergiants causes an apparent wind-absorption feature, increasingly cutting into the chromospheric emission with lower gravity. These two effects lead to an underestimate of the real chromospheric emission related to chromospheric magnetic heating on the upper RGB and AGB, which is increasing with lower gravity, when compared to what the respective *S*-index values, multiplied by their reference fluxes, would suggest.

To illustrate the Wilson–Bappu effect and its impact on the *S*-index determination, we show two example spectra of the Ca II K emission of θ_1 Tau, a K0 III giant in the Hyades (according to *Hipparcos*, $d = 46$ pc and $M_V = +0.5$), taken on 2015 November 10, and plotted in Fig. 1, and the spectrum of a typical K3 II giant (ι Aur, according to *Hipparcos*, $d = 151$ pc and $M_V = -3.2$), taken on 2015 November 12, and plotted in Fig. 2; both spectra were obtained with our robotic TIGRE telescope described in detail by Schmitt et al.

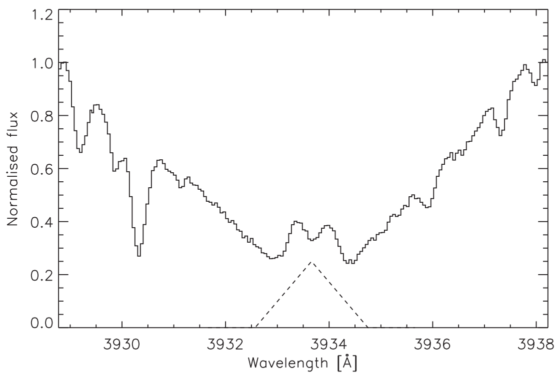

Figure 1. Chromospheric Ca II K emission of Hyades K0 III giant θ_1 Tau ($M_V = +0.5$) as observed with TIGRE. The width begins to exceed the narrow bandpass profile (indicated by the dashed triangle) of the *S*-index measurement.

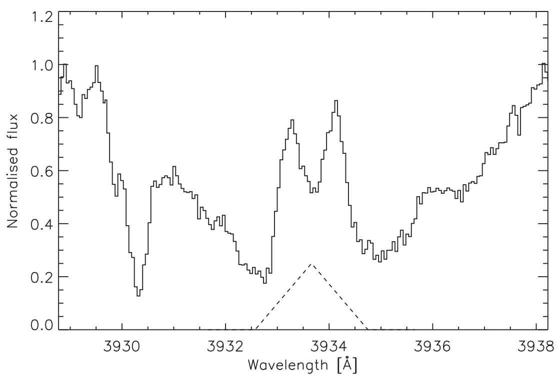

Figure 2. Chromospheric Ca II K emission of K3 II giant ι Aur ($M_V = -3.2$) as observed with TIGRE. As a result of the Wilson–Bappu effect, a significant fraction of the line emission of ι Aur falls outside the narrow bandpass profile used by the standard S-index.

(2014). The activity levels characterized in terms of the *S*-index of these stars are similar, and the *S*-index values obtained from our TIGRE measurements are 0.188 and 0.257, respectively, indicating elevated levels of magnetic activity. We note that both stars have also been detected at X-ray wavelengths – θ_1 Tau with the *Einstein Observatory* (Stern et al. 1981) and *ROSAT* survey observations (Stern, Schmitt & Kahabka 1995), and ι Aur in a deep *ROSAT* pointing (Kashyap et al. 1994) – at different emission levels (i.e. for θ_1 Tau an X-ray luminosity of $L_X \approx 10^{30}$ erg s^{-1} was measured, while ι Aur has $L_X \approx 1.8 \times 10^{27}$ erg s^{-1}, almost a thousand times weaker).

In Figs 1 and 2, we also indicate the narrow bandpass of the HK photometer (dashed triangle), to which we have calibrated our *S*-index values; see Rutten (1984) for a detailed discussion of the *S*-index bandpasses. It is immediately obvious that a substantial fraction of the Ca II K emission from the much brighter giant ι Aur falls outside the nominal window for *S*-index measurements.

Being well aware of this problem, the Mount Wilson team introduced a wider spectral window with a width of 1.5 Å around the Ca II H&K line cores, which was used for selected measurements after 1982 and which we refer to as the 'wide' bandpass. The latter issue is also addressed by Wilson (1982), who points out that for the brightest supergiants the emission core flux is missed even with this wide spectral window. Examining the *S*-index values for 125 giants, for which (non-simultaneous) measurements with both bandpasses are available in the Mount Wilson archive, we find that on average the *S*-index values based on the wide bandpass are increased by a factor of about 1.8 over the standard *S*-index derived from the narrow bandpass. This ought to be the resulting underestimate of the chromospheric emission by the *S*-index values for giants of luminosity class II and possibly even more for those of luminosity class I.

However, the wider emission-line bandpass was not the only change in the set-up for those alternative *S*-index measurements of the Mount Wilson team. The continuum reference bands also differ from those of the standard *S*-index used on these giants before 1982 and published by Duncan et al. (1991). Without knowing the exact calibration procedure of those wide bandpass measurements, it is currently difficult to compare and to interpret the respective *S*-index values in physical terms. In particular, the wider band picks up different photospheric contributions, and the numerical increase cannot be attributed to a more complete capture of the chromospheric emission alone.

We conclude from this discussion that the problem of smearing out of giant chromospheric emission by the Wilson–Bappu effect needs to be addressed by using a full measure of the Ca II emission, rather than mere *S*-index values, and a calibration of the spectral surface flux scale of the observed spectrum by the spectral fluxes of matching model atmosphere spectra.

3.3 From *S*-index data to an activity HR diagram

With the *S*-index data published by Baliunas et al. (1995), we have already demonstrated the scientific value of placing stars into the HR diagram to localize different degrees of activity (for main-sequence stars, see Schröder et al. 2013) and to link activity-related stellar properties to evolutionary status and mass. Here we expand this approach to all stars observed in the context of the Mount Wilson programme, including the most evolved cool giants.

Large parts of the first decades of the data collected in the framework of the Mount Wilson project have already been published by Duncan et al. (1991). Recently, the whole data base collected in the context of the Mount Wilson project has been made public and has become available to the astronomical community at large; the data can be downloaded from the web site ftp://solis.nso.edu/MountWilson_HK/, and a detailed description of the data is also provided there.

The available data specifically include the star identification, the calibrated *S*-index, which we use in this paper as the basis for our analysis, an instrument code indicating with which instrumental set-up the data were taken, and the date of the observation, as well as other material. The availability of this large data set extending over decades is a great asset for all studies of the rare and fast-evolving stages of stellar evolution, such as the far-evolved cool giants high on the RGB and AGB or the more massive cool giants.

Specifically, we find observations for almost 2300 different stars in the released Mount Wilson data base. Because we want to place the stars into the HR diagram, we demand a parallax accuracy of 10 per cent or better, which avoids misplacements by more than 0.2 mag. Most of these stars are located relatively nearby and are thus affected only little or even negligibly by interstellar absorption and extinction. Furthermore, we select only stars for which at least two measurements are available, and we always average the available observations. Here, we only consider entries where the instrument code contains the digit '1', which refers to the 'standard' 1.09-Å FWHM bandpass around the Ca II H&K lines, which we refer to as 'narrow' in the following. Note that additional data exist, which were taken with a wider bandpass, primarily used for observations of giant stars (see below); we refer to Duncan et al. (1991) for a description of the hardware to produce the data. In this way, we end up with a sample of 845 stars in total.

To relate these data to evolutionary states and masses, we place (see Fig. 3) the observed stars in the HR diagram, coded by the size of their respective *S*-index values; the colour/symbol coding in Fig. 3 is such that it visualizes fiducial low-activity stars (*S*-index below 0.2), modest-activity stars (0.2 to 0.3), enhanced-activity stars (between 0.3 and 0.4) and high-activity stars with different symbols and colours. For the HR diagram, we choose the observational coordinates M_V and $B - V$, and for comparison we plot the well-tested, calibrated evolutionary tracks based on the Cambridge Eggleton code, which for cool giants includes a detailed mass-loss description. For a detailed account of these evolution models and their calibration, as well as their transformation into an observational HR diagram, we refer to Schröder & Sedlmayr (2001) and Schröder & Pagel (2003), and further references therein.

Inspecting the post-main-sequence distribution of *S*-index values in Fig. 3 and the underlying evolutionary tracks – ignoring some individual cases of strong ($S > 0.6$) chromospheric emission, probably due to binarity, which distort the general picture – large *S*-index values are found among Hertzsprung-gap crossers, which are well known for their rejuvenated activity from their strong X-ray emission. By contrast, very modest-mass K clump giants and lower RGB stars show relatively low *S*-index values. Yet among the more luminous, more massive giants, we observe an increase of activity among He-burning stars in their blue loops; all these observations are fully consistent with what we already know about stellar activity from X-ray detections (Schröder et al. 1998).

The new and exciting feature demonstrated by Fig. 3 is the clear increase of the *S*-index values for stars higher up on the RGB and AGB with a colour redder than $B - V = 1.5$. This is demonstrated in the upper panel of Fig. 4, where we show stars with B_V colours in the range $1.5 < B - V < 1.6$ and $M_V < 1.S_{\rm MWO}$ versus M_V together with a formal linear regression. However, recalling the definition of the *S*-index as the ratio between the observed line-core emission in Ca II H&K and the photospheric flux $F_{\rm RV}$ in two nearby photospheric windows (R and V), and given the fact that the near-UV photospheric fluxes effectively decline with approximately the eighth power of effective temperature, an increase in $S_{\rm MWO}$ could be produced by a decrease in $T_{\rm eff}$ rather than an increase in chromospheric activity. Clearly we must convert the measured *S*-indices into energy fluxes to address this issue.

In order to check whether the clearly visible increase in the *S*-index with absolute magnitude and hence luminosity class among giants in the $B - V$ colour range $1.5 < B - V < 1.6$ is really associated with a rise of the actual chromospheric emission in terms of chromospheric emission-line surface fluxes, we must convert the observed *S*-indices into physical quantities. Rutten (1984) provides the empirical framework for this procedure. For all our sample stars, we have measurements of $S_{\rm MWO}$, $B - V$ and M_V, and we use Gray (2005) to derive empirical effective temperatures $T_{\rm eff}$ for all sample stars. The flux $F_{\rm HK}$ (in arbitrary units) in the Ca II line cores can then be computed from (note that this is equation 9 in Rutten 1984)

$$F_{\rm HK} = S_{\rm MWO} \times C_{\rm cf} \times T_{\rm eff}^4 \times 10^{-14}, \qquad (1)$$

where $C_{\rm cf}$ is a colour-dependent conversion factor given for giants in the relevant $B - V$ range (equation 10b in Rutten 1984) by the expression

$$\log C_{\rm cf} = 0.45 - 0.49(B-V) - 0.25(B-V)^2 - 0.066(B-V)^3. \qquad (2)$$

The fluxes $F_{\rm HK}$ computed in this way are shown in the second (from top) panel in Fig. 4; again, a clear increase indicated by a linear regression is visible.

Furthermore, Rutten (1984) derives a lower boundary $F_{\rm HK,\,min}$ for the observed flux $F_{\rm HK}$-distribution, which is displayed in his fig. 6; the corresponding values are listed in his table 2. From fig. 6(b) in Rutten (1984), we recognize a very smooth decrease of $F_{\rm HK,\,min}$ with $B - V$ colour. We interpret $F_{\rm HK,\,min}$ as the sum of the photospheric and basal flux contributions and we define an excess flux $\Delta F_{\rm HK}$ through the relation

$$\Delta F_{\rm HK} = F_{\rm HK} - F_{\rm HK,min}. \qquad (3)$$

This clearly suggests that we should interpret $\Delta F_{\rm HK}$ as the part of the flux $F_{\rm HK}$ that is related to magnetic activity. In the third panel (from top) in Fig. 4, we plot $\Delta F_{\rm HK}$ for our sample stars and the slope of the observed linear regression is even increased.

Finally, we can convert the excess fluxes $\Delta F_{\rm HK}$ derived in this way into physical units by introducing – following Mittag et al. (2013) – the quantity $R^+_{\rm HK}$ by defining

$$R^+_{\rm HK} = \frac{\Delta F_{\rm HK} \times 1.29 \times 10^6}{\sigma T_{\rm eff}^4}. \qquad (4)$$

In equation (4), σ denotes the Boltzmann constant and the factor 1.29×10^6 converts the fluxes $F_{\rm HK}$ into physical fluxes (in cgs units; see equation 11 in Rutten 1984 and his discussion). By definition, $R^+_{\rm HK}$ denotes the fraction of the total output in the Ca II line cores with respect to the bolometric output of the star and it represents a completely colour- and size-independent quantity to quantitatively characterize chromospheric activity.

In Fig. 4 (bottom panel), we plot the derived $R^+_{\rm HK}$-indices for our sample stars and we again recognize a clear increase in chromospheric activity with absolute magnitude. Therefore, we conclude that the observed increase in the *S*-index is indeed an increase of the chromospheric fluxes in the Ca II emission cores, rather than an artefact of the *S*-index definition. As shown in Section 3.2, a real chromospheric flux increase with luminosity might be larger than what is depicted here due to the Wilson–Bappu effect. We estimate that to make a factor of 1.5 or 2.

In summary, Fig. 4 demonstrates that the increase of chromospheric emission related to magnetic activity, as giants ascend on the giant branches, dominates over the falling photospheric reference fluxes across the respective narrow $B - V$ range. However, when we consider the wider $B - V$ range from already K3 subgiants (the coronal versus cool wind division; Hünsch et al. 1996) to M2 giants, then the decrease of the photospheric reference flux is larger than just across the narrower $B - V$ range of the giant branches. From about $B - V = 1.2$ with $C_{\rm cf} = 0.244$, $T_{\rm eff} \approx 4200$ K, to $B - V = 1.6$ with $C_{\rm cf} = 0.057$, $T_{\rm eff} \approx 3600$ K, the total decrease of the reference flux $F_{\rm RV}$ reaches a factor of the order of 8. In absolute terms, this almost compensates for most of the gains shown here to occur on the giant branches.

This means that the average rejuvenation of chromospheric magnetic heating around $B - V = 1.5$ mostly falls short of driving those late-giant chromospheres beyond the Athay point again, with only some exceptions formed by the most active cases. This is entirely consistent with observations. Indeed, several very active M-giants have been found with coronal X-ray emission (Hünsch et al. 1998),

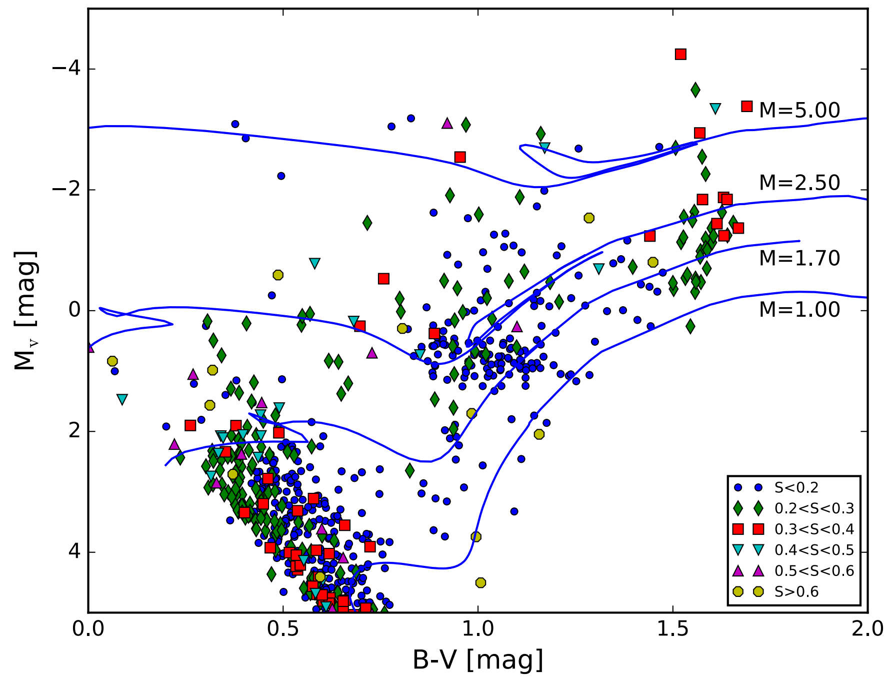

Figure 3. Sample stars from the Mount Wilson programme placed into an HR diagram, coded by S-index value strength using different symbols, for all stars with a relative parallax error better than 10 per cent. A general increase of chromospheric emission of evolved cool stars is notable on the the upper AGB around $B-V \approx 1.5$. Also shown are the evolutionary tracks for stars with various masses; see text for details.

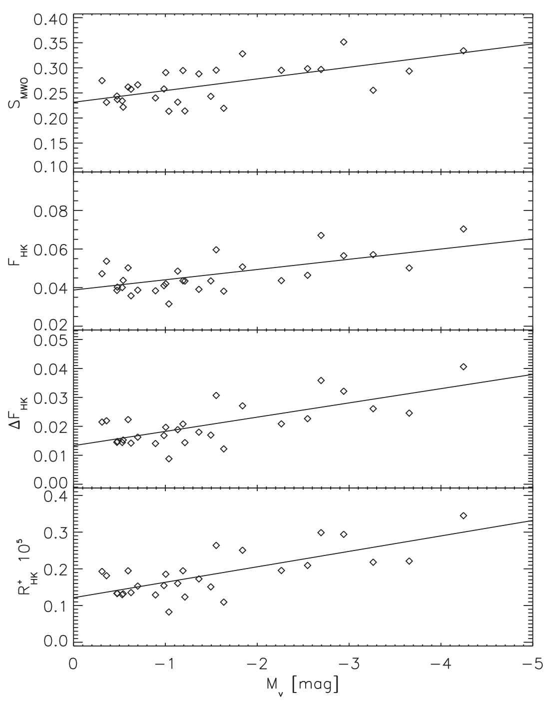

Figure 4. Top panel: $S_{\rm MWO}$ versus M_V for sample stars; a linear regression is plotted as a solid line. Second panel from top: same as top panel, but now the values of $F_{\rm HK}$ computed from equation (1) are shown. Third panel from top: same as top panel, but now the values of $\Delta F_{\rm HK}$ computed from equation (3) are shown. Fourth panel from top: same as top panel, but for $R^+_{\rm HK}$ values, computed from equation (4).

but these form a small minority among their kind. With this study of S-index values found in the HR diagram we can now show that these M-giants with coronal emission are not isolated phenomena, rather they form the tip of the proverbial 'iceberg'. There is a general rejuvenation of chromospheric magnetic heating in evolved giants around $B-V = 1.5$ seen in the rise of S-index values. Only in the most pronounced cases is this rise strong enough in absolute terms (considering the general decline of chromospheric heating among less cool giants) to drive the chromospheric material beyond the Athay point again.

4 DISCUSSION AND CONCLUSIONS

In our study of the chromospheric emission strength measured in the context of the Mount Wilson project, the S-index measurements for stars with an exact placement in the HR diagram combined with well-calibrated evolutionary tracks offer a new and clear picture of stellar activity in the course of late stellar evolution. On the coronal (i.e. hot) side of the Linsky–Haisch dividing line, this picture is fully consistent with the X-ray detections obtained since the 1980s. However, for the reasons detailed above, we argue that coronal X-ray emission is not representative for stellar activity on the cool side of the HR diagram, as the disappearance of coronae is a consequence of simple chromospheric physics. By contrast, both photospheric magnetic field measurements and chromospheric emission measurements are far less biased for the more evolved cool giants – and the latter (i.e. chromospheric emission) is much easier to observe.

Therefore, we are led to the conclusion that the initially declining stellar activity is not disappearing on the upper RGB and AGB, but it rather undergoes a significant revival during the last, more short-lived evolutionary stages of a cool, luminous giant. The rise of chromospheric Ca II H&K fluxes related to only magnetic heating is most significant, when shown over a luminosity scale.

This new finding can be understood in terms of a scenario suggested by asteroseismology – that the core contraction in the giant stages leads to a significant core spin-up. In fact, fast rotating cores have been proven to exist in Hertzsprung-gap-crossers and RGB stars, as they cause a splitting of bipolar, mixed (g- and p-) pulsation modes (Beck et al. 2012). The same argument ought to apply to AGB stars as well, which would naturally explain why in the meantime a large number of giants are known to show those split mixed modes (Buysschaert et al. 2012). Such fast rotating giant cores are expected to lead to strong, differential rotation of the outer convective envelope in radial direction. Also, such a fast spinning core might provide a type of dynamo to work in giant stars that differs from the solar dynamo, which in turn is based on differential rotation in latitude and thought not to work in the large convective envelopes of cool giants.

As stellar evolution speeds up on the most luminous segments of the RGB and AGB, viscosity-related braking in the interiors of these giant stars ought to become less important. Consequently, the contracting cores rotate even faster in the more luminous cool giants, and an even stronger radial rotational velocity profile is created. In these simple terms, we argue that it can be understood why the magnetic activity and chromospheric heating become stronger on the upper end of the giant branches. Furthermore, because stellar evolution in general proceeds much faster for larger masses, the same argument can be used to explain why the more massive stars are generally more active. Their evolution time-scales are a lot shorter and so compete much better with the time-scales of viscosity-related braking of the core.

In the future we plan to study the behaviour of giant stellar activity in the time domain to investigate this type of cool giant dynamo. For this purpose, it is necessary to monitor giant chromospheric emission over the time-scale of a decade or so. By obtaining the whole Ca II H&K line profile and comparing it with photospheric model atmospheres, which define the spectrally resolved surface flux scale, a measurement of the true chromospheric line emission fluxes will be possible, as well as quantitative studies of the temporal evolution of the giants' chromospheres.

ACKNOWLEDGEMENTS

We acknowledge the very helpful travel support from the bilateral project PROALMEX (CONACyT-DAAD) No. 207772, from the bilateral (CONACyT-DFG) grant No. 278156, as well as from CONACyT mobility grant No. 207662 (KPS), and by the DFG for several related projects. We use data from the venerable Mount Wilson Observatory HK Project, which ran from 1966 to 1992, and which was supported by both public and private funds through the Carnegie Observatories, the Mount Wilson Institute and the Harvard-Smithsonian Center for Astrophysics. This project owes its existence to the dedicated work of O. Wilson, A. Vaughan, G. Preston, D. Duncan, S. Baliunas, and many others. We also wish to thank the anonymous referee for making very valuable corrections to an earlier version of this publication.

REFERENCES

Athay G., 1981, ApJ, 250, 709

Athay R. G., Thomas R. N., 1956, ApJ, 123, 299

Aurière M. et al., 2015, A&A, 574, A90

Ayres T. R., Shine R. A., Linsky J. L., 1975, ApJ, 195, L121

Ayres T. R., Linsky J. L., Vaiana G. S., Golub L., Rosner R., 1981, ApJ, 250, 293

Ayres T. R., Brown A., Harper G. M., Bennett P. D., Linsky J. L., Carpenter K. G., Robinson R. D., 1997, ApJ, 491, 876

Ayres T. R., Brown A., Harper G. M., 2003, ApJ, 598, 610

Baliunas S. L. et al., 1995, ApJ, 438, 269

Beck P. G. et al., 2012, Nature, 481, 55

Buysschaert B. et al., 2016, A&A, 588, A82

Duncan D. K. et al., 1991, ApJS , 76, 383

Eberhard G., Schwarzschild K., 1913, ApJ, 38, 292

Gray D. F., 2005, The Observation and Analysis of Stellar Photospheres, 3rd edn. Cambridge University Press, Cambridge

Hubrig S., Plachinda S., Hünsch M., Schröder K.-P., 1994, A&A, 291, 890

Hünsch M., Schröder K.-P., 1996, A&A, 309, L51

Hünsch M., Schmitt J. H. M. M., Schröder K.-P, Reimers D., 1996, A&A 310, 801

Hünsch M., Schmitt J. H. M. M., Schröder K.-P., Zickgraf F.-J., 1998, A&A 330, 225

Kashyap V., Rosner R., Harnden F. R., Jr, Maggio A., Micela G., Sciortino S., 1994, ApJ, 431, 402

Konstantinova-Antova R. et al., 2013, Bulgarian Astronomical Journal, 19, 14

Linsky J. L., Haisch B. M., 1979, ApJ , 229, L27

Mittag M., Schmitt J. H. M. M., Schröder K.-P., 2013, A&A, 549, A117

Pérez Martínez M. I., Schröder K.-P., Cuntz M., 2011, MNRAS, 414, 418

Pérez Martínez M. I., Schröder K.-P., Hauschildt P., 2014, MNRAS, 445, 270

Perryman M. A. C., 2002, Ap&SS, 280, 1

Reimers D., 1982, A&A, 107, 292

Reimers D., Schmitt J. H. M. M., 1992, ApJ, 392, L55

Rutten R. G. M., 1984, A&A, 130, 353

Rutten R. G. M., Schrijver C. J., Lemmens A. F. P., Zwaan C., 1991, A&A, 252, 203

Schmitt J. H. M. M., 1997, A&A, 318, 215

Schmitt J. H. M. M. et al., 2014, Astron. Nachr., 335, 787

Schröder K.-P., 1990, A&A, 236, 165

Schröder K.-P., Pagel B. E. J., 2003, MNRAS, 343, 1231

Schröder K.-P., Sedlmayr E., 2001, A&A, 366, 913

Schröder K.-P., Hünsch M., Schmitt J. H. M. M., 1998, A&A, 335, 591

Schröder K.-P., Mittag M., Hempelmann A., González-Pérez J. N., Schmitt J. H. M. M., 2013, A&A, 554, A50

Stern R. A., Zolcinski M. C., Antiochos S. K., Underwood J. H., 1981, ApJ, 249, 647

Stern R. A., Schmitt J. H. M. M., Kahabka P. T., 1995, ApJ, 448, 683

Vaughan A. H., Preston G. W., Wilson O. C., 1978, PASP, 90, 267

Wilson O. C., 1967, PASP, 79, 46

Wilson O. C., 1978, ApJ, 226, 379

Wilson O. C., 1982, ApJ, 257, 179

Wilson O. C., Bappu M. K. V., 1957, ApJ, 125, 661

This paper has been typeset from a TEX/LATEX file prepared by the author.